MOLECULAR AND CELLULAR BIOLOGY, Mar. 1996, p. 1126–1137 Vol. 16, No. 3
0270-7306/96/$04.00+0

Cytoplasmic Sequestration of Wild-Type p53 Protein Impairs the G_1 Checkpoint after DNA Damage

UTE M. MOLL,[1]* ANNE G. OSTERMEYER,[1] ROBERT HALADAY,[1] BLONKA WINKFIELD,[1] MARK FRAZIER,[2] AND GERARD ZAMBETTI[2]

Department of Pathology, State University of New York at Stony Brook, Stony Brook New York 11794-8691,[1] and Department of Biochemistry, St. Jude Children's Research Hospital, Memphis Tennessee 38105[2]

Received 22 September 1995/Returned for modification 31 October 1995/Accepted 21 November 1995

Wild-type p53 protein is abnormally sequestered in the cytoplasm of a subset of primary human tumors including neuroblastomas (NB) (U. M. Moll, M. LaQuaglia, J. Benard, and G. Riou, Proc. Natl. Acad. Sci. USA 92:4407–4411, 1995; U. M. Moll, G. Riou, and A. J. Levine, Proc. Natl. Acad. Sci. USA 89:7262–7266, 1992). This may represent a nonmutational mechanism for abrogating p53 tumor suppressor function. To test this hypothesis, we established the first available in vitro model that accurately reflects the wild-type p53 sequestration found in NB tumors. We characterized a series of human NB cell lines that overexpress wild-type p53 and show that p53 is preferentially localized to discrete cytoplasmic structures, with no detectable nuclear p53. These cell lines, when challenged with a variety of DNA strand-breaking agents, all exhibit impaired p53-mediated G_1 arrest. Induction analysis of p53 and p53-responsive genes show that this impairment is due to suppression of nuclear p53 accumulation. Thus, this naturally occurring translocation defect compromises the suppressor function of p53 and likely plays a role in the tumorigenesis of these tumors previously thought to be unaffected by p53 alterations.

Wild-type p53 plays a key suppressor role in cell growth and tumor formation. p53 acts as a cell cycle checkpoint after DNA damage, induces G_1 arrest or apoptosis (reviewed in reference 63), and is required to maintain genomic stability (34, 70). The mechanism underlying its central growth suppression is largely based on p53's function as a potent transcriptional regulator (9, 13) of crucial growth-inhibitory genes such as *Waf-1*, a universal inhibitor of cyclin kinase complexes (10, 19, 47, 67). The domain structure of p53 reveals an N-terminal transactivation region, a central sequence-specific DNA-binding region, and a C-terminal oligomerization region that also harbors several nuclear localization domains (reviewed in reference 50). Accordingly, p53 is a nuclear phosphoprotein, and nuclear localization is essential for its growth-suppressing activity in late G_1 (14, 15, 53–56). Site-directed mutagenesis of the primary nuclear localization signal (at residues 316 to 322) caused cytoplasmic retention and completely destroyed the transformation-suppressing activity of wild-type p53 (56). In normal cells, p53 levels are tightly regulated as a result of a short half-life of 15 to 30 min (49) and are not detectable by immunocytochemistry (31).

Disruption of the p53 response pathway strongly correlates with tumorigenesis. Indeed, functional inactivation of p53 is the single most common event in human malignancies and occurs in at least 50% of all cancers (20). Mutational inactivation is the most common mechanism and occurs in a large spectrum of sporadic and familial cancers of, e.g., the breast, gastrointestinal tract, lung, brain, and soft tissues (22). Deletion of one allele accompanied by a missense mutation in the central DNA-binding domain of the remaining allele is classical. Most point mutations prolong the half-life of p53, leading to nuclear accumulation which now becomes readily detectable by immunocytochemistry. Though less frequent, mutation-independent mechanisms are also utilized in human malignancies. Here, the common theme is sequestration of wild-type p53 protein by another protein which abrogates its suppressive action. Originally, this was discovered in mammalian models of viral oncogenesis. The viral oncoproteins simian virus 40 large T antigen and adenovirus type 5 E1B form stabilized complexes with p53, thereby functionally inactivating it (6, 40, 68). In human papillomavirus-positive genitoanal cancers, the high-risk human papillomavirus type 16 and type 18 E6 oncoproteins form a p53 complex resulting in rapid p53 degradation (52). Additional oncoviral proteins that complex with p53 include hepatitis B virus X protein, associated with hepatocellular carcinoma (11, 60, 62), and cytomegalovirus IE84 protein, associated with smooth muscle proliferation in coronary restenosis (57). Furthermore, in 30% of soft-tissue sarcomas, p53 is inactivated by binding to the overexpressed product of the *mdm-2* oncogene, which inhibits p53-mediated transactivation (44, 48).

Recently, we described a potential mutation-independent mechanism of p53 inactivation which involves abnormal cytoplasmic sequestration of wild-type p53 with concomitant nuclear exclusion. This phenotype was present in 37% of inflammatory breast carcinomas and greater than 95% of undifferentiated neuroblastomas (NB) but never in differentiated benign derivatives of NB (42, 43). To answer the crucial question about p53 function in this phenotype, we show here that such tumor cells have indeed severely impaired or abolished p53 function. To do this, we characterized the first available in vitro model derived from four different human NB tumors and subjected them to various types and degrees of DNA damage. Although these cells grossly overexpress wild-type p53 protein, the p53-mediated G_1 checkpoint response to lower and medium-range DNA damage is either severely impaired or abolished altogether as a result of its cytoplasmic sequestration.

* Corresponding author. Mailing address: Department of Pathology, State University of New York at Stony Brook, Stony Brook, NY 11794-8691. Phone: (516) 444-2459. Fax: (516) 444-3424. Electronic mail address: umoll@Path.SOM.Sunysb.edu.

Thus, this naturally occurring translocation defect compromises the suppressor function of p53 in the DNA damage pathway and likely plays a role in the oncogenesis of these tumors, which were previously thought to be unaffected by p53 alterations, as judged by their wild-type p53 gene status.

MATERIALS AND METHODS

Cells and reagents. Established human tumor cell lines were used, and cells were cultured in RPMI 1640–10% heat-inactivated fetal calf serum or Dulbecco's modified Eagle medium–10% fetal calf serum (MDA lines and H 358) at 37°C in 5% CO_2. p53-overexpressing SK-N-SH, LAN-5, IMR-32, and CHP 134 are derived from undifferentiated NB. p53-deficient lines SK-N-MC and CHP 100 are derived from neuroepitheliomas, which are closely related, primitive neuroectodermal malignancies (all a gift from Jeffrey Marks and available from the American Type Culture Collection). The H 358 lung adenocarcinoma line harbors a homozygous deletion of p53 (59). The ML-1 myeloid leukemia line harbors normal levels of wild-type p53 (25). Breast cancer lines MDA 468 and MDA 231 are homozygous for an R273H and an R280K mutation, respectively. Antibodies to p53 were monoclonal antibodies PAb 421, 1801, and 240 (Oncogene Science), DO-1 (Santa Cruz Biotechnology), and PAb 248 (69). The four monoclonal antibodies recognize different p53 epitopes: amino acids 32 to 79 (PAb 1801), 210 to 219 (PAb 240), 157 to 192 in the mouse (PAb 248), and 17 to 26 (DO-1). PAb 240 reacts equally well with mutant and wild-type p53 in fixed tissue (42, 69). In immunoprecipitation experiments, p53 was detected by immunoblotting with CM-1, a rabbit polyclonal antibody against bacterially expressed human wild-type p53 (gift of David Lane). Heat shock protein was detected with monoclonal hsp72/73 (Santa Cruz Biotechnology). Waf-1 was detected by a rabbit polyclonal serum against recombinant human Waf-1 protein (gift of David Beach). mdm-2 protein was detected with a rabbit polyclonal serum against the C-terminal half of mouse mdm-2 that cross-reacts with human mdm-2 (gift of Arnold Levine). Mouse 3T3 DM cells were used as positive control for mdm-2 overexpression (gift of Donna George). Nuclear antigens were detected with monoclonal antibodies against proliferating cell nuclear antigen (PCNA) (Oncogene Science), Ki-67 antigen (Dako), or MIB-1 (a recombinant part of the Ki-67 antigen) (AMAC Inc.). Monoclonal LAMP-1 (University of Iowa Hybridoma Bank) (2) served as a lysosomal marker. Baculovirus-produced human wild-type p53, either crude or highly purified, was used as the control in various assays.

Immunoblotting and immunoprecipitation. For immunoblotting, cells from confluent P_{100} dishes were scraped and lysed in 100 μl of radioimmunoprecipitation assay buffer (10 mM Tris [pH 7.4], 150 mM NaCl, 1% sodium deoxycholate, 1% Triton X-100, and 0.5% sodium dodecyl sulfate [SDS] plus a protease inhibitor cocktail consisting of 2 μg of aprotinin per ml, 2 μg of leupeptin per ml, and 1 mM phenylmethylsulfonyl fluoride). Equal amounts of supernatant (50 μg of total protein per lane) were electrophoresed through SDS–8% polyacrylamide gels and blotted onto a nitrocellulose membrane overnight at 100 mA in transfer buffer (1× Laemmli buffer, 10% methanol, 0.01% SDS). The membrane was blocked in 3% milk in TBST (10 mM Tris [pH 8], 44 mM NaCl, 0.05% Tween 20) for 1 h, washed three times in TBST, and incubated in mouse monoclonal antibodies at indicated dilutions for 1 h. After three washes in TBST, the blot was incubated for 1 h in biotinylated anti-mouse antibody (1:2,500; Amersham ECL kit), washed again, and developed as instructed by the manufacturer.

For immunoprecipitation, scraped cell pellets were sonicated in 300 μl of TENN buffer (50 mM Tris [pH 7.4], 5 mM EDTA, 0.5% Nonidet P-40, 150 mM NaCl, protease inhibitors). After centrifugation at 14,000 rpm for 30 min, the supernatant was precleared with 30 μl of protein G-agarose beads (Gibco BRL). Equal amounts of total protein (750 μg) were precipitated with 1.5 μg of PAb 421 for 2 h. The beads were washed three times in SNNTE (50 mM Tris [pH 7.4], 5 mM EDTA, 5% sucrose, 1% Nonidet P-40, 0.5 M NaCl) and one time with radioimmunoprecipitation assay buffer. Samples were solubilized by boiling in SDS-polyacrylamide gel electrophoresis running buffer before being loaded onto a gel.

Immunofluorescence. Cells were grown on polylysine-coated coverslips, rinsed in phosphate-buffered saline, fixed for 3 min in acetone-methanol (1:1), and air dried. We strictly used this nonaqueous fixative to avoid any possible artifactual shift in subcellular p53 localization as has been described for when fixatives with >30% water content are used (17). After blocking in 10% normal goat serum for 20 min, the cells were incubated in primary antibody (mouse) for 2 h. Staining was detected with biotinylated goat anti-mouse immunoglobulin G (IgG) followed by streptavidin-fluorescein isothiocyanate (Gibco BRL). Cells were mounted with Antifade (Molecular Probes) and examined with a Nikon confocal scanning laser microscope. For p53 immunofluorescence after actinomycin D (Act D) treatment, cells were preplated for 24 h before the drug was added for an additional 24 h. A cell was scored as positive as soon as nuclear staining could be discerned. For each condition, at least 3,000 cells were counted in each of two to three independent experiments. Autofluorescence background was minimal and easily distinguished by a yellow-reddish quality.

DNA sequencing. Total RNA was extracted from SK-N-SH, LAN-5, IMR-32, and CHP 134 cells and reverse transcribed with random hexamers. Full-length p53 cDNA was PCR amplified from codons 1 to 148, 118 to 353, and 253 to 393. PCR products were gel purified, and both strands of each amplicon (400 ng) were directly sequenced with the fluorescent DyeDeoxy sequencing kit (Applied Biosystems) and run on an automated DNA sequencer (ABI model 370A). Control tumor cDNA with known missense mutations in the central amplicon, amplified and sequenced in parallel, readily yielded detectable mutant nucleotides.

Northern (RNA) blot analysis. Cells were exposed to a single dose of X irradiation (X-IR) (1 to 4 Gy at 150 kV/3 mA) in a Minishot 160 Irradiator. Following irradiation, the cells were returned to the incubator for 6 h before harvesting. Total cellular RNA was prepared by using RNAzol (Tel-Test) as described by the manufacturer. The RNA (10 μg per lane) was electrophoresed through 1.5% agarose–6% formaldehyde gels prepared in MOPS buffer {20 mM MOPS (3-[*N*-morpholino]propanesulfonic acid; pH 7.0), 5 mM sodium acetate, 1 mM EDTA, 3.7% formaldehyde}. The RNA was transferred to Zeta-Probe nylon membranes in 20× SSC (1× SSC is 0.15 M NaCl plus 0.015 M sodium citrate), and the filters were baked at 80°C for 1 h under vacuum and prehybridized for 3 h at 42°C in the hybridization buffer (50% formamide, 5× SSC, 5× Denhardt's buffer, 1% dextran sulfate, 20 μg of bovine serum albumin per ml, 50 mM sodium phosphate [pH 7.0], 0.5% SDS, 125 μg of sheared salmon sperm DNA per ml). Hybridization was performed for 18 to 24 h at 42°C with thermally denatured, radiolabeled cDNAs encoding human Waf-1 and mdm-2 (pHDM and pZL-WAF 1 were gifts from Bert Vogelstein) at 2×10^6 cpm/ml. Filters were exposed to XAR-5 film (Kodak), and signals were quantitated by PhosphorImager analysis using ImageQuant software (Molecular Dynamics).

Fluorescence-activated cell sorting (FACS) analysis. For each datum point, 3×10^6 cells were preplated into P_{100} dishes for 24 h in RPMI 1640–10% fetal calf serum and then either not treated or treated for an additional 24 h (dose response) or up to 24 h (time response) with Act D (0.45, 1.8, and 7.2 nM; Sigma) and bleomycin (0.06 U; Bristol-Myers Squibb) added to the medium for the indicated times. X-IR (1, 2, and 4 Gy; Minishot 160) and ^{137}Cs γ irradiation (δ-IR) (0.5 and 1 Gy; Gammator M; Isomedix Inc.) were pulse delivered before cells were returned to the incubator for the indicated times. Cells were collected with trypsin-EDTA and stained for DNA content with propidium iodide (Sigma) as described previously (64). Cell fractions were analyzed on a Becton Dickinson FACScan, using R and S models of Cell Fit software. Each graph represents three to seven experiments. Results are expressed as percent change in G_0/G_1 and S fractions of treated versus untreated cells for each cell line.

Subcellular fractionation. Cells from four dishes (175 cm^2) were scraped in ice-cold HS buffer (10 mM *N*-2-hydroxyethylpiperazine-*N*′-2-ethanesulfonic acid [HEPES; pH 7.4], 250 mM sucrose, 2 μg of aprotinin per ml, 2 μg of leupeptin per ml, 1 mM phenylmethylsulfonyl fluoride, 20 mM NaF, 1 mM sodium orthovanadate) and centrifuged at 1,000 rpm for 2 min. As indicated, in some experiments HS buffer included 1% Nonidet P-40 or 1% Triton X-100. The cell pellet was resuspended in 5 ml of HS buffer and carefully homogenized in a Dounce homogenizer (tight fit; Wheaton) until 50 to 70% of the cells were broken up. The homogenate was centrifuged twice at 1,000 *g* for 10 min. The $1,000 \times g$ pellets were pooled, and the supernatant was laid on top of 5 ml of HS buffer in a polyallomer tube containing 55% sucrose and centrifuged overnight at $100,000 \times g$ at 20°C. After the spin, three layers were discernible: the top 3 ml of cloudy material, representing the membrane pellet, was collected and pelleted by an additional $100,000 \times g$ spin for 1 h (16). The sucrose supernatant and sucrose pellet were collected directly. All three fractions were dialyzed in 2 liters of HS buffer and concentrated to 300 μl. Of each fraction, 150 μg of total protein was loaded onto an SDS–8% polyacrylamide gel and immunoblotted with DO-1 (0.1 μg/ml). For enzyme treatments, the $1,000 \times g$ supernatants were split and incubated for 30 min at 37°C with or without trypsin (1:50 [wt/wt]) or RNase A (10 μg/ml) before further processing.

RESULTS

Overexpressed wild-type p53 in NB cells is sequestered in the cytoplasm. Guided by our previous finding of sequestered p53 in primary human NB and a report by Davidoff et al. (5) which described overexpression of wild-type p53 in immunoprecipitates from whole cell extracts of NB cell lines, we reasoned that these NB lines would provide an excellent model for the phenotype present in vivo. Under normal culture conditions, the four NB lines SK-N-SH, LAN-5, IMR-32, and CHP 134 show constitutive overexpression of p53 compared with the classic cell line ML-1, a myeloid leukemia line which contains normal low levels of functional wild-type p53 (Fig. 1). ML-1 cells had previously been critical in identifying the G_1 arrest activity of p53 (25). In contrast, two control lines derived from NB-related neuroepitheliomas contain abnormally low levels of full-length p53 protein as a result of aberrant size (SK-N-MC) or stability (CHP 100) of their p53 transcripts (5) and

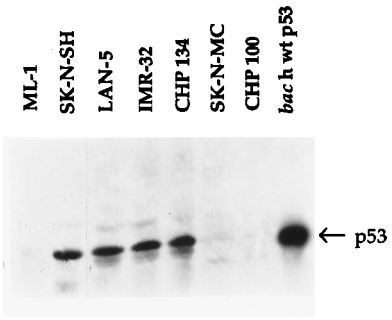

FIG. 1. Wild-type p53 is overexpressed in human NB cell lines. The immunoblot was probed with p53-specific monoclonal antibody DO-1 (0.1 μg/ml) (50 μg of whole cell extract per lane). The control cell line ML-1 contains normal (low) levels of wild-type p53 and is barely detectable. SK-N-MC and CHP 100 have abnormally low levels of p53 protein. Baculovirus recombinant human wild-type p53 (*bac* h wt p53) is shown for comparison.

completely lack any induction of p53 or p53-responsive gene products, even when maximally induced by DNA-damaging agents (see Fig. 7B to F for CHP 100; data not shown for SK-N-MC), indicating that the residual p53 in these two lines is nonfunctional. Homozygous wild-type status of the p53 gene was shown by full-length cDNA sequencing in SK-N-SH, IMR32, and CHP 134 as well as exon 5 to 9 sequencing in the remaining line (data not shown) and is consistent with our previous sequencing data on primary NBs (42).

Localization studies using fluorescence and alkaline phosphatase-based immunocytochemistry with four different p53-specific monoclonal antibodies showed that p53 was strictly localized to the cytoplasm in 100% of the cells present in the culture (Fig. 2), with no detectable protein in the nucleus. This was true for all four NB lines. Moreover, while some cytoplasmic p53 staining showed a diffuse character, p53 preferentially localized to punctated, discrete structures that were randomly dispersed throughout the cytoplasmic compartment (Fig. 2A; see also Fig. 7A). This pattern was most conspicuous with PAb 1801 and 248. CHP 100, which expresses abnormally low levels of p53, yielded only occasional cytoplasmic dots (Fig. 2A). The punctated p53 pattern, while vaguely reminiscent of a lysosomal pattern, was distinctly different from the staining pattern with the LAMP-1 antibody, a marker for lysosomes (Fig. 2B). In contrast, breast carcinoma cells that harbor p53 missense mutations at codon 273 (MDA 468) and codon 280 (MDA 231) exhibit the well-described nuclear accumulation of p53 (Fig. 2B and data not shown). This punctate p53 localization is in contrast to the MCF-7 breast cancer line, which shows only diffuse cytoplasmic p53 and had been the only previously recognized cell line with cytoplasmically sequestered wild-type p53 (58). Furthermore, p53 sequestration in MCF-7 cells is leaky and possibly cell cycle dependent, leading to a mixture of cells with cytoplasmic and/or nuclear overexpression in exponentially growing cultures (45). Some investigators even find it exclusively in the nucleus and only in a few percent of the cells (65), suggesting that distinct sublines of MCF-7 may exist.

The aberrant sequestration in NB cells appears specific for p53, since other proteins that are destined to move to the nucleus, such as PCNA, Ki-67, and MIB-1, are translocated properly (Fig. 3A). Since certain forms of p53 are known to complex with HSP70 family members (4, 21), we investigated whether the punctated cytoplasmic p53 is colocalized with HSP72/73. However, the staining pattern obtained with an hsp72/73 antibody was discordant and characterized by a homogeneous distribution involving both nucleus and cytoplasm (Fig. 3B). Furthermore, while NB cells express higher levels of total HSP72/73 protein than do ML-1 cells, as seen by Western blot (immunoblot) analysis (Fig. 3C), only a minute portion is complexed with p53, as shown by immunoprecipitation (Fig. 3D). Thus, we excluded heat shock protein as a component that sequesters p53 within the cytoplasm. Previously we showed that the *mdm-2* gene is not amplified in primary NB (42). In addition, immunoblotting of NB cells failed to show detectable levels of *mdm-2*, excluding *mdm-2* deregulation (reviewed in reference 1) as a possible (although unlikely) source of cytoplasmic retention of p53 (data not shown).

Sequestered p53 is preferentially localized in large protein aggregates. The conspicuous immunofluorescence pattern suggested that we should be able to physically capture the cytoplasmic p53 structures. We therefore performed partition experiments (Fig. 4). NB cells were fractured in a detergent-free buffer. After unbroken cells as well as nuclei associated with various amounts of adherent cytoplasmic fragments were spun out (Fig. 4, low spin P fraction), the cytoplasmic fraction was subjected to ultracentrifugation through stringent sedimentation conditions (high-density 55% sucrose cushion). This technique separates the cytoplasm into membrane-bound vesicles with high buoyancy (M fraction), soluble cytosolic proteins (SN fraction), and pelletable large protein aggregates (P fraction) (16). Indeed, analysis of the P and M fractions by conventional electron microscopy showed greater than 98% purity of both fractions. The P fraction consisted of amorphous granular protein aggregates, while the M fraction contained closed, circular membrane profiles representing membrane-bound vesicles of various types (data not shown). This finding indicates that our fractionation technique did not cause artifacts by severing the integrity of cytoplasmic vesicles. Consistent with its apparent size and shape, the cytoplasmic p53 partitioned virtually exclusively to the 100,000 × *g* pellet (Fig. 4A, lane 2), with only a minute amount detectable in the M fraction (lane 4) and a complete absence in the SN fraction (lane 3). This fractionation profile is specific for NB cells, since the nuclear p53 overexpressor line MDA 468, containing mainly soluble p53 tetramers and perhaps dimers, shows a mirror image profile. In MDA 468 cells, p53 partitioned to the SN fraction (lane 7) but not to the P fraction (lane 6). The same is true for highly purified recombinant p53 that was subjected to sucrose ultracentrifugation (lanes 9 and 10). The small amount of p53 detectable in the M fractions (Fig. 4A, lanes 4, 8, and 11; Fig. 4B, lane 3; Fig. 4C, lanes 4 and 8) probably represents endoplasmic reticulum-associated p53. (On the other hand, minor contamination during fraction collection, although care was taken to avoid it, cannot be ruled out.) When we repeated the experiment with LAN-5 cells, this time including 1% Nonidet P-40 or 1% Triton X-100 in the lysis buffer, the results were identical, suggesting that the pelletable p53 is not easily solubilized (data not shown). This p53-pelletable material is sensitive to trypsin digestion (Fig. 4B; compare lanes 1 to 3 with lanes 4 to 6), again confirming its membrane-free nature. Cytoplasmic p53 has been reported to be covalently linked to 5.8S rRNA (12). If this were the case here, one would expect p53 to partition to the soluble fraction after RNase A treatment. We excluded this possibility by repeating the experiment in the presence or absence of prior RNase A treatment. Figure 4C shows that the partition profile remains the same with or without RNase A (compare lanes 1 to 4 with lanes 5 to 8). Taken together, these results demonstrate that sequestered p53 in NB cells localizes to large, free protein aggregates in the cytoplasm.

Cytoplasmic sequestration of p53 results in functional impairment of the p53-mediated G_1 checkpoint after DNA damage. To directly test if the aberrant location of wild-type p53

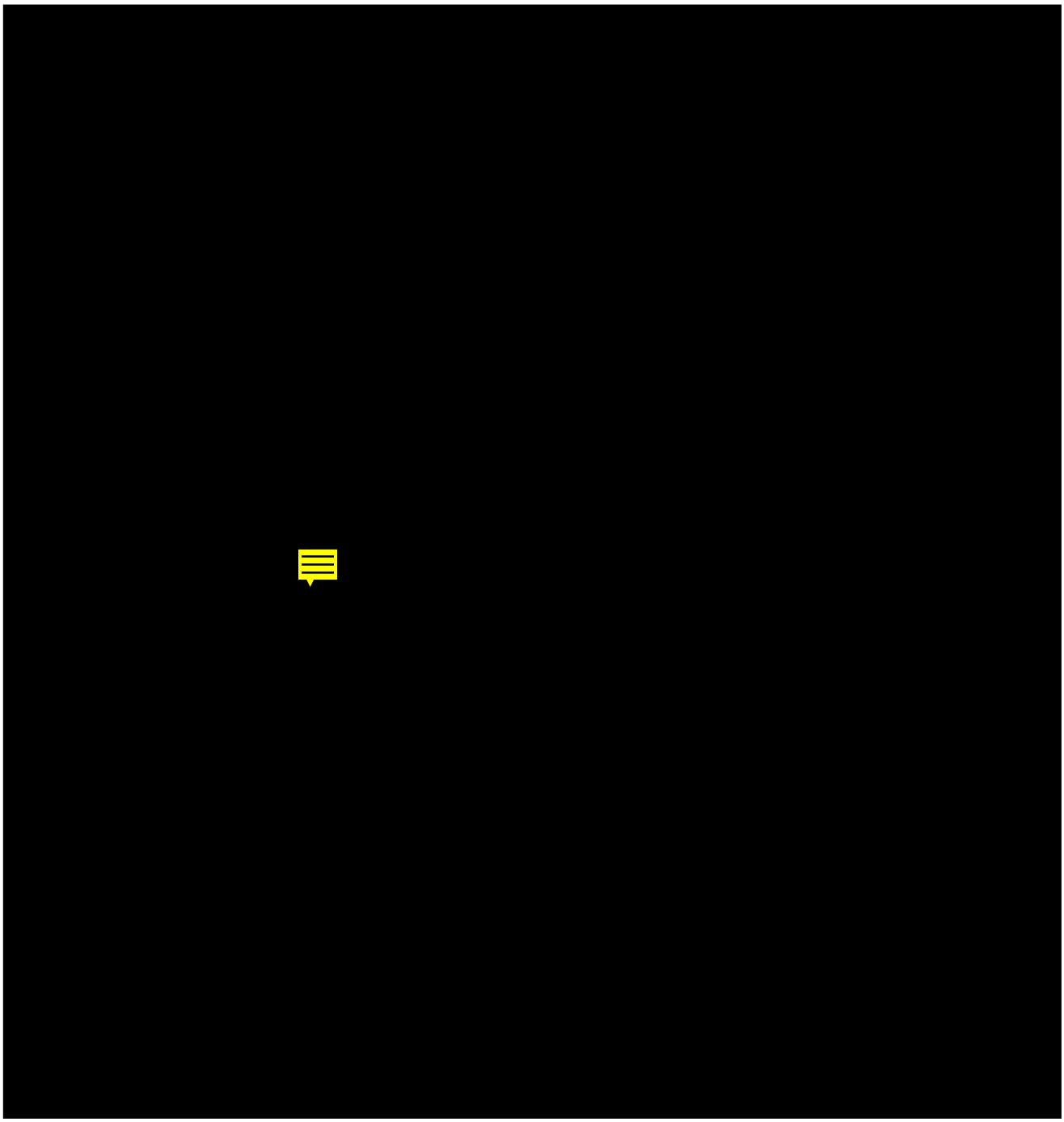

FIG. 2. p53 is preferentially localized to discrete structures in the cytoplasm but is absent from the nucleus. (A) Immunofluorescence of NB lines (SK-N-SH [SH], LAN-5, IMR-32, and CHP 134) and a p53-deficient control line (CHP 100) with p53-specific monoclonal antibodies. Fluorescein isothiocyanate-based localization with PAb 1801 (0.5 μg/ml) or PAb 248 (hybridoma supernatant) is shown. A similar localization is obtained with alkaline phosphatase-fast red detection, here shown with DO-1 (0.5 μg/ml) and PAb 240 (2 μg/ml). Because of a higher amplification factor in the enzyme-based technique, the staining appears more intense and confluent. The four monoclonal antibodies recognize different p53 epitopes (see Materials and Methods). (B) Controls were stained with normal mouse IgG (0.5 μg/ml) instead of p53 antibodies. For comparison, MDA 468 breast cancer cells (R273H mutation) show the typical nuclear accumulation. The cytoplasmic p53 structures are unrelated to lysosomes, as judged from the discordant pattern with LAMP-1, a lysosomal marker antibody. The scale bar equals 15 μm.

compromises its normal biological activity, we analyzed the G_1 checkpoint function of p53 after DNA damage, using FACS (Fig. 5 and 6). When the NB cells (SK-N-SH, LAN-5, IMR-32, and CHP 134) were challenged with DNA strand-breaking agents such as Act D (Fig. 5A), X-IR (Fig. 5B and 6), ^{137}Cs γ-IR (Fig. 5C), and bleomycin (data not shown), cell cycle analysis showed that all lines exhibit markedly impaired G_1 arrest for most or all agents in comparison with the positive control line ML-1. In fact, the response of SK-N-SH to low and moderate levels of DNA damage was virtually indistinguish-

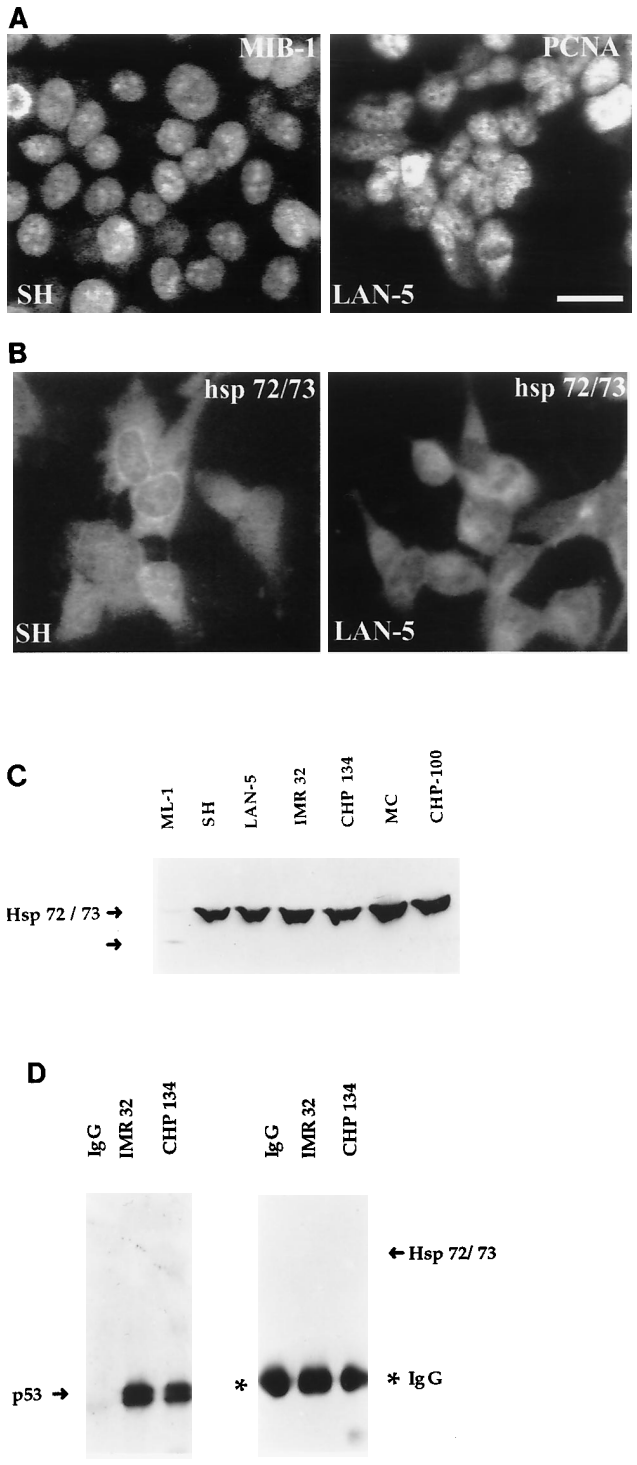

FIG. 3. (A) Cytoplasmic sequestration in NB cells is specific for p53. Other proteins that are destined to translocate to the nucleus, such as PCNA, MIB-1, and Ki-67 (data not shown), are readily detected in the nucleus. Shown is immunofluorescence of SK-N-SH and LAN-5 cells with antibodies against nuclear markers MIB-1 (4 μg/ml) and PCNA (2 μg/ml). The scale bar equals 15 μm for panels A and B. (B to D) Heat shock protein is not responsible for cytoplasmic retention of p53. (B) Immunofluorescence of SK-N-SH and LAN-5 cells with HSP72/73 antibody (1 μg/ml) yields a diffuse distribution throughout the cell that is unrelated to that of p53. (C) Immunoblot with equal amounts of whole cell extract (50 μg per lane) was probed with HSP72/73. ML-1 shows four faint but distinct bands, two of which are below the 60-kDa range. SH, SK-N-SH; MC, SK-N-MC. (D) Immunoprecipitation with PAb 421 (1.5 μg) from 1 mg of whole cell extract or buffer (lanes labeled IgG). The material was split in half and immunoblotted for p53 (rabbit CM-1; left) and HSP72/73 (mouse monoclonal antibody; right). The original blot shows a very faint heat shock band indicating only minimal complex formation with p53. Note that IgG heavy chains and p53 migrate at the same rate.

able from responses of the p53-deficient lines (SK-N-MC, CHP 100, and H 358) with all types of DNA-damaging treatments. Importantly, Act D was used in the nanomolar range as previously described (7, 29) as opposed to the micromolar range within which it acts as a general transcriptional inhibitor. Act D treatment of the other three lines showed an intermediate response for LAN-5 and IMR-32 and a quasi-normal response for CHP 134 (Fig. 5A). It is of note that Act D damage in these experiments was cumulative because of the drug's continuous presence in the culture medium for 24 h. This differs from the pulse damage delivered by X-IR and γ-IR. In addition, Act D causes DNA strand breaks indirectly by irreversibly complexing with topoisomerase II, thereby fixing the transient double-strand breaks that are created by topoisomerase II (46). Since the individual topoisomerase II levels are likely to vary among the different cell lines that we studied, the seemingly normal response of CHP 134 to Act D might be due to very high levels of topoisomerase II in this line, producing excessive numbers of strand breaks. To circumvent this complex situation, we therefore reexamined the arrest response with X-IR, γ-IR, and bleomycin, all of which cause strand breaks directly (46) (Fig. 5B and C, Fig. 6, and data not shown). Under these conditions, LAN-5, IMR-32 and CHP 134 all showed severe failure to arrest, and SK-N-SH was again unable to arrest. Apoptosis did not occur in this system, as determined by morphology and cell viability tested by the trypan blue exclusion assay (data not shown).

The response of SK-N-SH to Act D and X-ray damage was extensively characterized for the induction of p53 protein as well as p53-responsive gene products such as Waf-1 (10, 19, 47, 67), gadd45 (26) (data not shown), and mdm-2 (24, 66), using Northern, Western, and immunofluorescence analyses (Fig. 7). The results are in excellent agreement with the FACS data (Fig. 5 and 6). On a cellular level, ML-1 cells showed a dose-dependent vigorous p53 induction, with 0, 31, and 91% of total cells exhibiting detectable nuclear p53 protein (exclusively nuclear) at 0, 0.45, and 1.8 nM Act D, respectively (Fig. 7A). In contrast, under the same conditions, SK-N-SH exhibited a severe suppression of nuclear accumulation of p53, with only 0, 1.5, and 7% p53-positive nuclei at the same concentration range (Fig. 7A). Importantly, the great majority of cells failed to respond. That some cells did induce nuclear p53 probably reflects the fact that DNA damage is a stochastic event and that, possibly cell cycle dependent, some cells sustain a greater degree of injury and therefore induce higher levels of p53 than the rest. Presumably, those were the cells that arrested properly in G_1, which is reflected by a slight drop in the S fraction with a reciprocal slight increase in the G_1 fraction (Fig. 5A). The cells that did induce nuclear p53 consistently exhibited a concomitant increase of cytoplasmic p53, from a limited number of p53 dots when untreated to several hundred when exposed to Act D (Fig. 7A). This result suggests that the cytoplasmic retention mechanism is saturable, and when its retention capacity for induced p53 protein is exceeded during severe DNA damage, excess p53 eventually overflows and enters the nucleus, where it is fully active in transactivating its targets. This prediction was confirmed when we exposed SK-N-SH cells to superhigh levels of Act D (7.2 nM). Now, the system became responsive, with over 90% of the SK-N-SH cells ex-

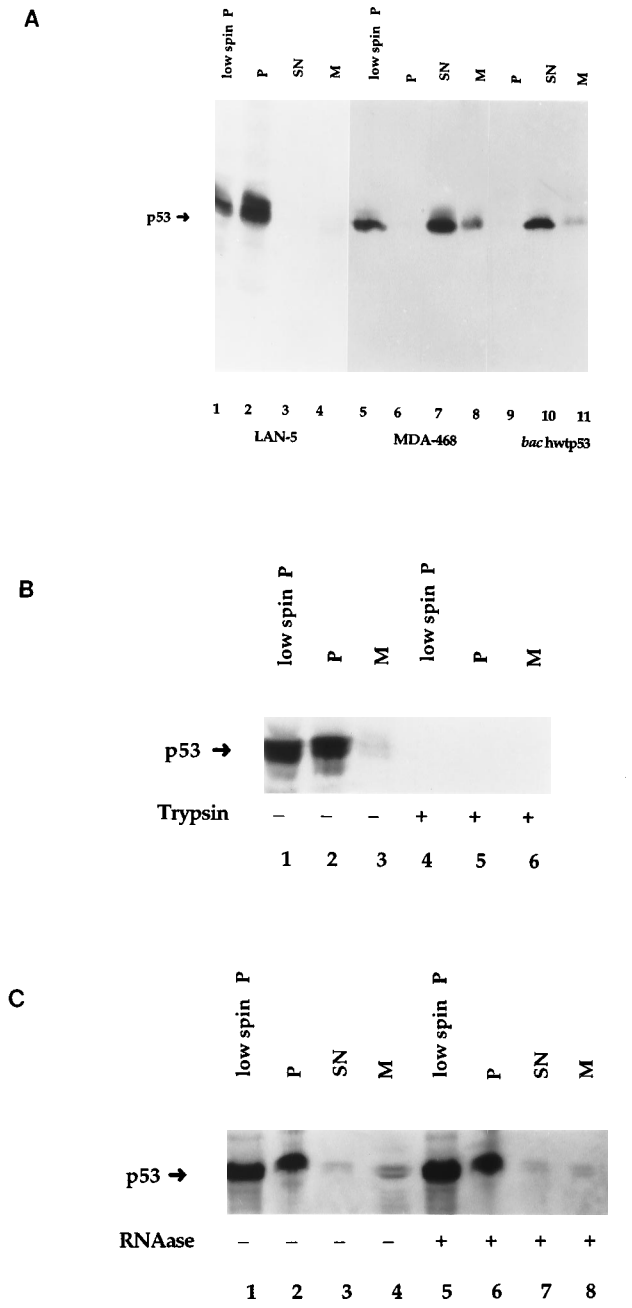

FIG. 4. Sequestered p53 localizes to large, free protein aggregates in the cytoplasm. (A) LAN-5 (lanes 1 to 4) and MDA 468 (lanes 5 to 8) cells were homogenized, and their 1,000 × *g* supernatants as well as purified wild-type p53 (*bac* hwt p53; lanes 9 to 11) were subjected to 55% sucrose ultracentrifugation as described in Materials and Methods. (B) The pelletable p53 species is trypsin sensitive. LAN-5 homogenates were split in half and either treated (lanes 4 to 6) or mock treated (lanes 1 to 3) with trypsin before fractionation as described in for panel A. (C) Cytoplasmic RNA is not associated with this p53 species. LAN-5 preparations as used for panel B were treated (lanes 5 to 8) or mock treated (lanes 1 to 4) with RNase A. Equal amounts (150 μg of total protein) of P, SN, and M fractions were immunoblotted with DO-1 in all panels.

hibiting nuclear p53 (Fig. 7A, SH/ 7.2). At the same time, the cytoplasmic p53 dots increased dramatically, again suggesting that the cytoplasmic retention activity of p53 is saturable.

The immunofluorescence data were confirmed by immunoblot and Northern analyses of p53 and its downstream targets *Waf-1* and *mdm-2*, using lysates of treated and untreated cells (Fig. 7B to F). While Act D-mediated p53 induction in ML-1 was 40-fold (L, 0.45 nM) and 54-fold (H, 1.8 nM), SK-N-SH only showed 1.3- and 2.0-fold induction, respectively, whereas CHP 100 was completely unresponsive (Fig. 7B). Importantly, the induction profile of *Waf-1* transcripts with 0.45 and 1.8 nM Act D (Fig. 7C) paralleled that of p53 protein (compare Fig. 7B and C). ML-1 showed 5.1- and 19.1-fold increases of *Waf-1* mRNA, in contrast to SK-N-SH, which showed suppressed responses of 0.96 (none) and 3.4-fold, respectively. A Western blot for Waf-1 protein confirmed the mRNA data, ML-1 showed 5.4- and 11.3-fold induction and SK-N-SH showed 1.0- and 2.3-fold induction at 0.45 and 1.8 nM Act D, respectively (data not shown). Together with the immunofluorescence data, this finding further supports the conclusion that nuclear localization is essential for p53 function (14, 15), 53–56). We noted that SK-N-SH is the only one of the four NB lines that contained detectable *Waf-1* mRNA and protein when untreated (Fig. 7C). To definitively eliminate the possibility of very low levels of functionally active, albeit undetectable, nuclear p53 in these cells, we generated stable NB lines that harbor a human wild-type p53-responsive chloramphenicol acetyltransferase reporter gene (COS×1CAT) that was previously used (66). Two of two independently derived SK-N-SH clones and four of four LAN-5 clones failed to show any activity when untreated, as measured by a sensitive chloramphenicol acetyltransferase enzyme-linked immunosorbent assay (41). This finding further confirms nuclear exclusion of p53 in NB cells. Taken together with the G_1 checkpoint data, it suggests that SK-N-SH cells have some p53-independent baseline *Waf-1* expression which has also been described for other cell lines (32, 39). Northern analysis for Act D-induced *mdm-2* yielded identical results, while *gadd45* transcripts showed partial p53 independence since they were present at low levels in untreated SK-N-SH cells and p53-deficient cells (data not shown).

Agreement between functional and biochemical data is also seen with X-ray damage (compare Fig. 5B and 6A with Fig. 7D to F). p53 induction 6 h after exposure to 0, 1, 2, and 4 Gy was vigorous in ML-1 cells but severely suppressed in LAN-5, IMR-32, and CHP 134 cells (Fig. 7D). Again, after X-ray damage, NB cells show a severe suppression of p53 induction which is associated with impaired G_1 arrest. As seen for Act D, *mdm-2* mRNA induction parallels the p53 protein induction rather well (Fig. 7D and F). Interestingly, in SK-N-SH cells, the X-ray-mediated *mdm-2* induction is even more suppressed than the Act D-mediated *Waf-1* induction (compare Fig. 7C and E).

DISCUSSION

The experiments presented here demonstrate for the first time that (i) cytoplasmic retention of wild-type p53 in NB cells results in severe functional impairment of the p53-mediated G_1 checkpoint response (this defect is most pronounced at lower levels of DNA damage); (ii) the cytoplasmic retention activity is saturable; (iii) when the retention capacity for induced p53 protein is eventually exceeded during severe damage, excess p53 overflows and enters the nucleus, where it is fully active in transactivating its target genes; and (iv) sequestered p53 is preferentially localized to discrete cytoplasmic structures consistent with large protein aggregates.

This p53 translocation phenotype occurs naturally in a distinct subset of human tumors. We originally observed it in over one-third of inflammatory breast carcinomas, which are epithelial tumors, and over 95% of undifferentiated NB, which are neural crest-derived tumors. This finding led us to postulate

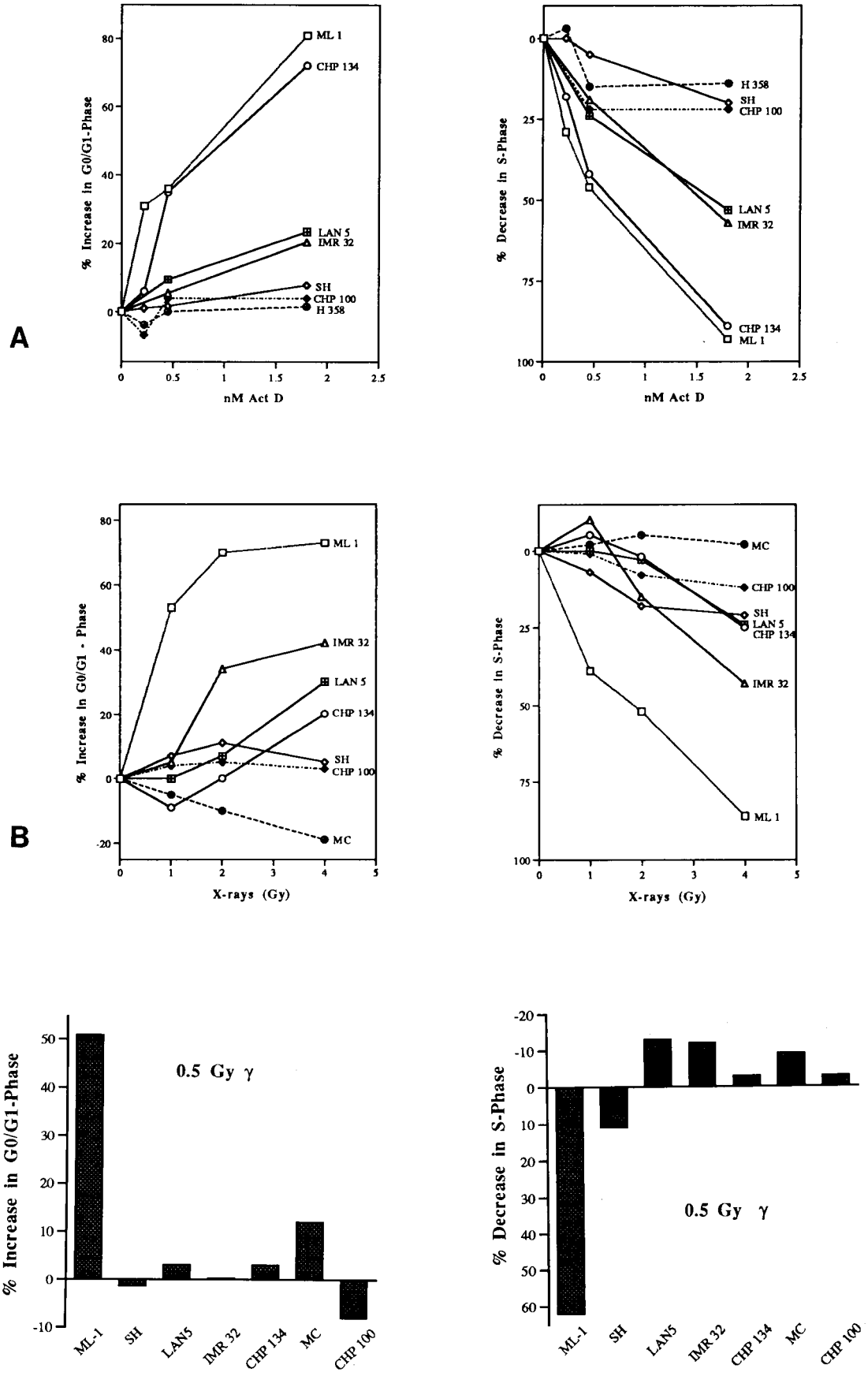
A
% Increase in G0/G1-Phase
nM Act D
ML 1
CHP 134
LAN 5
IMR 32
SH
CHP 100
H 358
% Decrease in S-Phase
nM Act D
H 358
SH
CHP 100
LAN 5
IMR 32
CHP 134
ML 1
B
% Increase in G0/G1 - Phase
X-rays (Gy)
ML 1
IMR 32
LAN 5
CHP 134
SH
CHP 100
MC
% Decrease in S-Phase
X-rays (Gy)
MC
CHP 100
SH
LAN 5
CHP 134
IMR 32
ML 1
C
% Increase in G0/G1-Phase
0.5 Gy γ
ML-1
SH
LAN5
IMR 32
CHP 134
MC
CHP 100
% Decrease in S-Phase
0.5 Gy γ
ML-1
SH
LAN5
IMR 32
CHP 134
MC
CHP 100

FIG. 5. Aberrant cytoplasmic localization of wild-type p53 severely impairs the p53-mediated G_1 checkpoint after DNA damage. FACS analysis of propidium iodide-labeled cells was performed as described in Materials and Methods. After challenge with DNA strand-breaking agents such as Act D (A), X-IR (B), or ^{137}Cs γ-IR (C), NB cells exhibit a severely impaired G_1 arrest response to most or all agents compared with ML-1 cells, which have functional p53 that mediates a proper G_1 arrest response. This is most pronounced in the lower dose range. Results are expressed as percent change in G_0/G_1 (left) and S (right) fractions of treated versus untreated cells for each cell line after 24 h of exposure. SH, SK-N-SH; MC, SK-N-MC.

that this phenotype may represent a nonmutational mechanism for abrogating p53 suppressor function. To test this hypothesis, we have established an in vitro model that accurately reflects the p53 sequestration found in vivo. This system allowed us to test the functional consequences of this phenomenon. We show here that sequestration of p53 impairs the major cell cycle checkpoint after DNA damage, thus severely compromising the p53 tumor suppressor function in NB cells. This is most pronounced at lower levels of DNA damage which might be the physiologically relevant ones that operate during tumorigenesis of malignant neoplasms. Excellent agreement exists between results that we obtained from extensive analysis of three different sets of parameters: cell cycle analysis, p53 localization, and the induction of p53 and 53-responsive genes. Our results provide a cellular basis for some long-known observations. Clinically, it is well established that NB tumors are highly radiosensitive, making radiotherapy a major treatment modality (18, 27). Likewise, undifferentiated human NB cell lines are unusually radiosensitive (8, 23, 33, 37). In fact, high UV radiation sensitivity of NB cells was associated with very low DNA repair activity. In addition, low doses of UV induce little or no postirradiation inhibition of DNA replication (23). In view of our findings, the most attractive explanation for these observations is that NB cells lack the G_1 checkpoint as a result of p53 inactivation (sequestration), therefore rapidly accumulating and propagating mutagenic lesions that lead to mitotic failure and (nonapoptotic) cell death (30). Conversely, p53 sequestration may be reversible. Aberrant p53 sequestration is intimately associated with failure to differentiate. In contrast, differentiation of NB cells is associated with downregulation of overexpressed p53 to normal cellular levels (5, 42, 51), a concomitant conversion of the sequestered phenotype to the wild-type phenotype both in differentiated benign derivative tumors of primary neuroblastoma (42) and in vitro (41) and, importantly, a dramatic rise in the ability to undergo apoptosis (28, 38, 41). This differentiation-associated conversion suggests a possible reconstitution to functional p53.

Our experiments used ML-1 cells as a positive control. This cell line is a logical choice because it harbors normal levels of functional wild-type p53, shows a wild-type p53 phenotype, is well characterized with respect to its p53-dependent G_1 arrest response, and is rather reactive to DNA damage (25). We did not perform clonogenic assays. However, given the high susceptibility to damage in NB cells (33), it appears unlikely that the impaired G_1 arrest that we observed is simply due to an intrinsic hyporesponsiveness of NB cells compared with ML-1 cells; rather, it likely reflects authentic differences in their abilities to react to the same damage.

Perhaps the most intriguing result is that the cytoplasmic retention activity of p53 showed saturable properties and is associated with conspicuous punctate structures. Our biochemical characterization strongly suggests that these structures represent large, cytosolic protein aggregates that appear insoluble. These structures are not associated with membrane-bound vesicles, as evident by their partitioning into the nonmembranous pellet fraction under detergent-free conditions and their sensitivity to trypsin digestion. Normal p53 undergoes cell cycle-dependent translocation. In growth-stimulated, synchronous populations of nontransformed BALB/c 3T3 cells, the newly synthesized p53 accumulates in the cytoplasm during the G_1 phase, when it rises from undetectable levels (at 0 h) to detectable levels (at 6 h) but remains excluded from the nucleus. Just prior to the G_1/S transition, a relatively rapid translocation into the nucleus occurs (at 8 h), where it remains for about 3 h during initiation of DNA synthesis. Subsequently, there is a redistribution back into the cytoplasmic compartment associated with gradually declining levels (53). Similar results were seen with rat embryo fibroblasts transfected with *ras* and a temperature-sensitive p53 Val-135 mutant (15, 36). This cell cycle-associated compartmentalization indicates that p53 activity is tightly regulated through spatial and temporal availability, in addition to overall cellular levels. Seemingly, this spatial regulation went awry in tumors with the translocation defect and appears stuck in one position. Heat shock

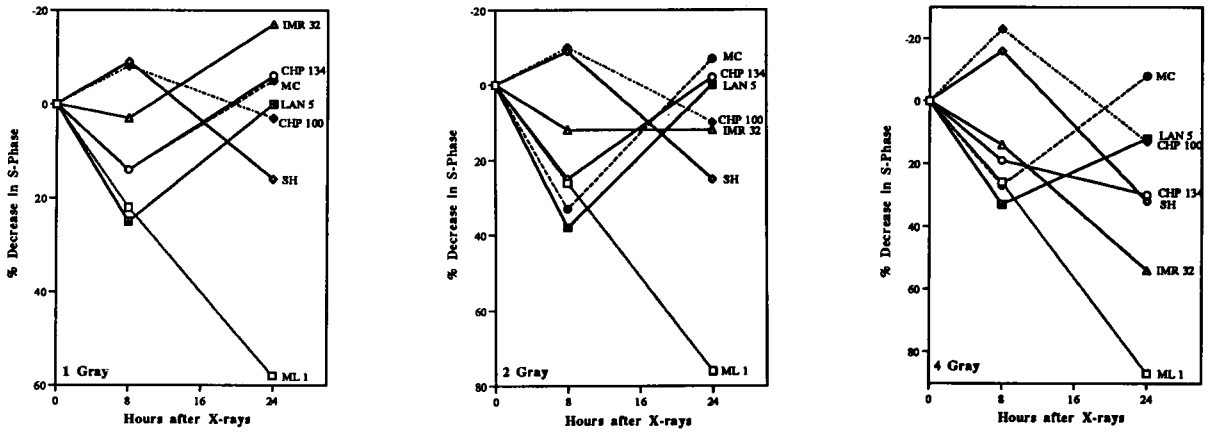

FIG. 6. Time dependence of the G_1 arrest response after 1, 2, and 4 Gy X-IR. The functional impairment of sequestered p53 is also apparent when analyzed in a time-dependent fashion. Similar results were obtained with γ-IR (data not shown). The kinetics are consistent with reported data (34). FACS analysis as was performed for Fig. 6.

FIG. 7. DNA damage-mediated induction of nuclear p53 and p53-transactivated gene products is severely suppressed in NB cells. (A) Immunofluorescence with PAb 1801 of ML-1 cells (upper row) and SH cells (lower four panels) after 24 h of incubation in 0, 0.45, and 1.8 nM Act D. The values represent the fractions of total cells with detectable nuclear p53. ML-1 shows a vigorous nuclear p53 induction, with 91% positive nuclei at 1.8 nM Act D. In contrast, SH cells are strongly suppressed, with only 7% positive nuclei at the same concentration. A superhigh dose (7.2 nM) eventually induces a full response in SH cells. Concomitant with nuclear p53 induction, a marked increase in the number of cytoplasmic p53 structures is a consistent feature. (B and C) Protein analysis of p53 (B) and mRNA analysis of Waf-1 (C) from cells treated with 0 (C), 0.45 nM (L), and 1.8 nM (H) Act D for 24 h. The p53 induction profile parallels the imaging data in panel A. SH cells are severely suppressed in inducing p53 and p53-responsive gene products. Similarly, X-ray treatment fails to induce adequate p53 protein levels (D) and *mdm-2* mRNA levels (E and F). Cells were harvested 6 h after exposure to 0, 1, 2, or 4 Gy. Kinetic studies determined the peak p53 protein induction at 6 h after X-IR in ML-1 and NB cells (data not shown). (B and D) Immunoblots of cell lysates (50 μg per lane) were probed with DO-1. (C, E, and F) Northern blots (10 μg of total RNA per lane) were probed with a ^{32}P-labeled human *Waf-1* or *mdm-2* cDNA. The fold induction values determined by PhosphorImager analysis are indicated below the lanes (B to E) or depicted in graphic form (F; C [0 Gy], 1 [1 Gy], 2 [2 Gy], and 4 [4 Gy]).

proteins can serve as chaperones that anchor certain steroid receptors and protein kinases to the cytoskeleton. Upon binding of the ligand, the receptor is released from the cytoplasmic anchor and enters the nucleus, where it functions in transcriptional regulation. HSP70 proteins have previously been demonstrated to complex with mutant and wild-type p53 (4, 21). We found no significant p53-HSP70 complex formation in NB lines, indicating that the cytoplasmic sequestration of p53 is not dependent on this class of molecular chaperones. What could be the nature of the punctate p53 structures and how are they formed? Several possibilities need to be considered. It is conceivable that a putative p53-specific nuclear transporter is lacking in these cells. Currently, there is no firm evidence for the existence of such a dedicated transport molecule. Alternatively, sequestered p53, although wild type in its coding sequence, might have undergone an aberrant posttranslational modification that interferes with its nuclear access. However, the fact that severe DNA damage, in addition to the sequestered pool, induces a p53 species that is no longer retained but instead translocates properly to the nucleus strongly argues against both of these possibilities. Could the large p53 aggregates consist of misfolded waste protein, perhaps made up of thousands of p53 monomers that render them resistant to protease digestion as has been described for other proteins (61)? Again, the fact that a properly translocating second species is made under conditions of high p53 production argues

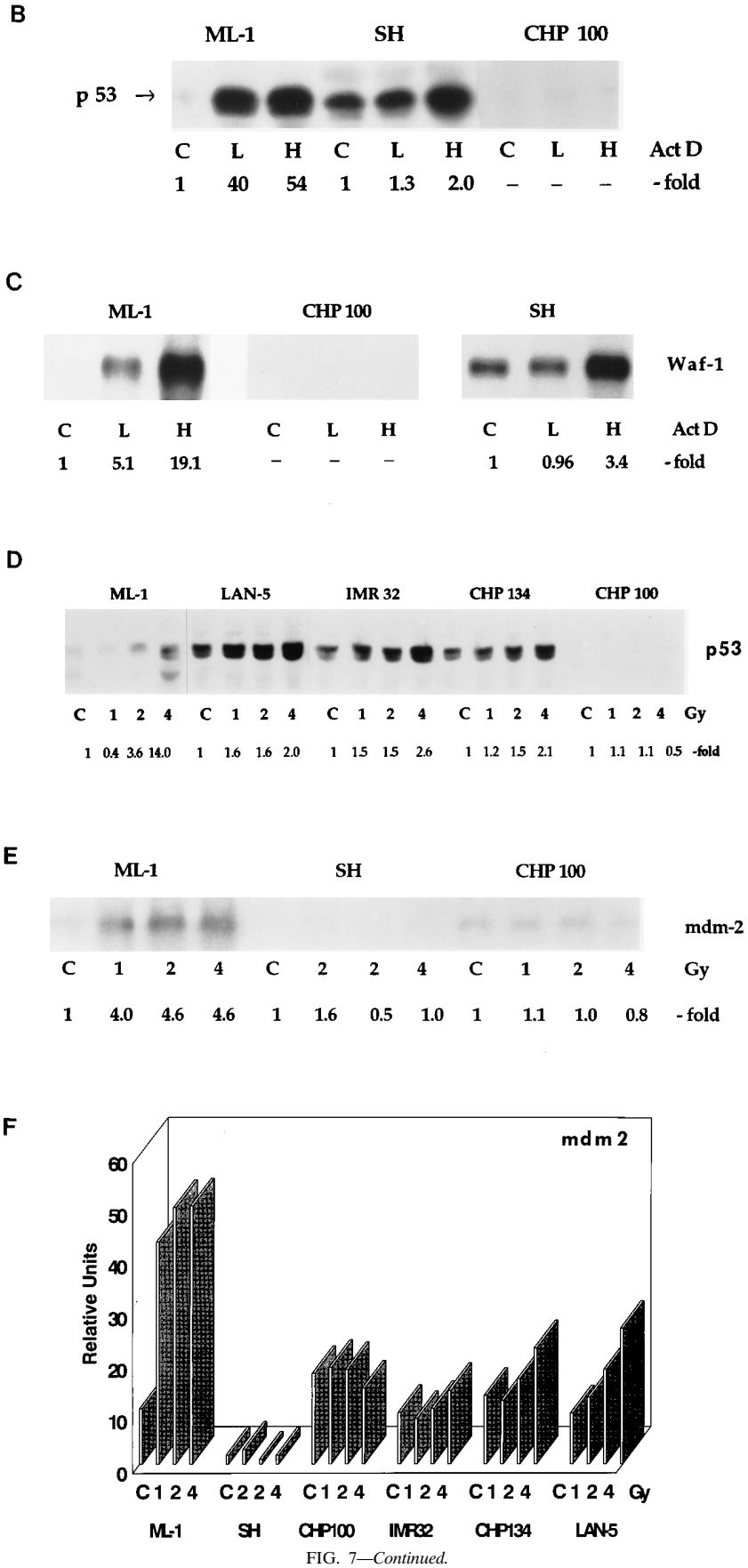

FIG. 7—*Continued.*

against this idea. Possibly the most attractive speculation emerging from our data is that a titratable cytoplasmic anchor protein, perhaps a chaperone, which is available in limited amounts forms large multimeric complexes with p53. Once all of the available binding sites are occupied, p53 is no longer trapped and is free to move. In keeping with this model, binding to this anchor would protect p53 from degradation at this site. Support for the anchor model comes from stable SK-N-SH transfectants that overexpress the C-terminal p53 peptide. In five of five independent clones, the endogenous p53 translocates to the nucleus as a heterocomplex (41a). This anchor could be an exaggerated version of a physiological regulator of p53, in which case these NB lines could help to elucidate p53 regulation in normal cells. Alternatively, it could represent a tumor cell-specific aberrant protein.

In summary, we have shown that cytoplasmic sequestration of wild-type p53 is the principal mechanism of p53 inactivation in undifferentiated NB. Identifying the molecular pathology will be the next important step. Given the vast clinical potential of reconstituting the transcriptional activity of p53 in human tumors, this wild-type p53 phenotype appears to be a promising candidate for such therapeutic efforts.

ACKNOWLEDGMENTS

This work was supported by Public Health Service grant CA60664-01 from the National Cancer Institute (to U.M.M.), by American Cancer Society grant JFRA-477 (to U.M.M.), by Cancer CORE grant 5P30-CA21765 (to G.Z.), and by the ALSAC of St. Jude Children's Research Hospital (G.Z.).

We thank Erik Runko and Brand Ahn for excellent technical assistance and Peter Tegtmeyer for purified baculovirus-made p53 and critical reading of the manuscript.

ADDENDUM

The *BRCA1* gene product, a putative transcription factor encoded by the familial breast/ovarian cancer suppressor gene, has recently been localized to the cytoplasm of sporadic breast cancer cells (3). This abnormality is reminiscent of the one in p53 that we have described here.

REFERENCES

1. **Bueso-Ramos, C. E., T. Manshouri, M. A. Haidar, Y. O. Huh, M. J. Keating, and M. Albitar.** 1995. Multiple patterns of MDM-2 deregulation in human leukemias: implications in leukemogenesis and prognosis. Leukemia Lymphomas **17:**13–18.
2. **Chen, J. W., Y. Cha, K. U. Yuksel, R. W. Gracy, and J. T. August.** 1988. Isolation and sequencing of a cDNA clone encoding lysosomal membrane glycoprotein mLAMP-1; sequence similarity to proteins bearing onco-differentiation antigens. J. Biol. Chem. **263:**8754–8758.
3. **Chen, Y., C.-F. Chen, D. J. Riley, D. C. Allred, P.-L. Chen, D. Von Hoff, C. K. Osborne, and W.-H. Lee.** 1995. Aberrant subcellular localization of BRCA 1 in breast cancer. Science **270:**789–791.
4. **Davidoff, A. M., J. D. Iglehart, and J. R. Marks.** 1992. Immune response to p53 is dependent upon p53/HSP 70 complexes in breast cancers. Proc. Natl. Acad. Sci. USA **89:**3439–3442.
5. **Davidoff, A. M., J. C. Pence, N. A. Shorter, J. D. Iglehart, and J. R. Marks.** 1992. Expression of p53 in human neuroblastoma- and neuroepithelioma-derived cell lines. Oncogene **7:**127–133.
6. **Debbas, M., and E. White.** 1993. Wild-type p53 mediates apoptosis by E1A which is inhibited by E1B. Genes Dev. **7:**546–554.
7. **Demers, W., S. A. Foster, C. L. Halbert, and D. A. Galloway.** 1994. Growth arrest by induction of p53 in DNA damaged keratinocytes is bypassed by human papillomavirus 16 E7. Proc. Natl. Acad. Sci. USA **91:**4382–4386.
8. **Eady, J. J., and J. H. Peacock.** 1992. Host cell reactivation of gamma-irradiated adenovirus 5 in human cell lines of varying radiosensitivity. Br. J. Cancer **66:**113–118.
9. **El-Deiry, W. S., S. E. Kern, J. A. Pietenpol, K. W. Kinzler, and B. Vogelstein.** 1992. Definition of a consensus binding site for p53. Nat. Genet. **1:**45–49.
10. **El-Deiry, W. S., T. Tokino, V. E. Velculescu, D. B. Levy, R. Parsons, J. M. Trent, D. Lin, E. Mercer, K. W. Kinzler, and B. Vogelstein.** 1993. WAF 1, a potential mediator of p53 suppression. Cell **75:**817–825.
11. **Feitelson, M. A., M. Zhun, L. X. Duan, and W. T. London.** 1993. Hepatitis B X antigen and p53 are associated in vitro and in liver tissues from patients with primary hepatocellular carcinoma. Oncogene **8:**1109–1117.
12. **Fontoura, B. M. A., E. A. Sorokina, E. David, and R. B. Carroll.** 1992. P53 is covalently linked to 5.8S rRNA. Mol. Cell. Biol. **12:**5145–5151.
13. **Funk, W. D., D. T. Pak, R. H. Karas, W. E. Wright, and J. W. Shay.** 1992. A transcriptionally active DNA binding site for human p53 protein complexes. Mol. Cell. Biol. **12:**2866–2871.
14. **Gannon, J. V., and D. P. Lane.** 1991. Protein synthesis required to anchor a mutant p53 protein which is temperature-sensitive for nuclear transport. Nature (London) **349:**802–806.
15. **Ginsberg, D., D. Michael-Michalovitz, D. Ginsberg, and M. Oren.** 1991. Induction of growth arrest by a temperature-sensitive p53 mutant is correlated with increased nuclear localization and decreased stability of the protein. Mol. Cell. Biol. **11:**582–585.
16. **Green, J., G. Griffith, D. Louvard, P. Quinn, and G. Warren.** 1981. Passage of viral membrane proteins through the Golgi complex. J. Mol. Biol. **152:**663–698.
17. **Gusterson, B. A., R. Anbazhagan, W. Warren, C. Midgely, D. P. Lane, M. O'Hare, A. Stamps, R. Carter, and H. Jayatilake.** 1991. Expression of p53 in premalignant and malignant squamous epithelium. Oncogene **6:**1785–1789.
18. **Halperin, E. C., and E. B. Cox.** 1986. Radiation therapy in the management of neuroblastoma: the Duke University Medical Center experience from 1967–1984. Int. J. Radiat. Oncol. Biol. Phys. **12:**1829–1837.
19. **Harper, J. W., G. R. Adam, N. Wei, K. Keyomars, and S. J. Elledge.** 1993. The p21 Cdk-interacting protein Cip 1 is a potent inhibitor of G1 cyclin-dependent kinases. Cell **75:**805–816.
20. **Harris, C. C., and M. Hollstein.** 1993. Clinical implication of the p53 tumor suppressor gene. N. Engl. J. Med. **329:**1318–1327.
21. **Hinds, P. W., C. A. Finlay, A. B. Frey, and A. J. Levine.** 1987. Immunological evidence for the association of p53 with a heat shock protein, hsc70, in p53-plus-*ras*-transformed cell lines. Mol. Cell. Biol. **7:**2863–2869.
22. **Hollstein, M., K. Rice, M. S. Greenblatt, T. Soussi, R. Fuchs, T. Sorlie, E. Hovig, B. Smith-Sorensen, R. Montesano, and C. C. Harris.** 1994. Database of p53 gene somatic mutations in human tumors and cell lines. Nucleic Acids Res. **22:**3551–3555.
23. **James, M., and J. Mansbridge.** 1982. Ultraviolet radiation sensitivity of proliferating and differentiated human neuroblastoma cells. Int. J. Radiat. Biol. **41:**547–556.
24. **Juven, T., Y. Barak, A. Zauberman, D. L. George, and M. Oren.** 1993. Wild type p53 can mediate sequence-specific transactivation of an internal promoter within the mdm2 gene. Oncogene **8:**3411–3416.
25. **Kastan, M. B., O. Onyekwere, D. Sidransky, B. Vogelstein, and R. W. Craig.** 1991. Participation of p53 protein in the cellular response to DNA damage. Cancer Res **51:**6304–6311.
26. **Kastan, M. B., Q. Zhan, W. S. El-Deiry, F. Carrier, T. Jacks, W. V. Walsh, B. S. Plunkett, B. Vogelstein, and A. J. Fornace, Jr.** 1992. A mammalian cell cycle checkpoint pathway utilizing p53 and gadd 45 is defective in ataxia telangiectasia. Cell **71:**587–597.
27. **Koop, C. E., and L. Schnaufer.** 1975. The management of abdominal neuroblastomas. Cancer **35:**905–909.
28. **Kruman, I. I., M. A. Kostenko, R. Y. Gordon, V. I. Popov, and S. R. Umansky.** 1993. Differentiation and apoptosis of murine neuroblastoma N1E115. Biochem. Biophys. Res. Commun. **191:**1309–1318.
29. **Kulesz-Martin, M. F., B. Lisafeld, H. Huang, N. D. Kisiel, and L. Lee.** 1994. Endogenous p53 protein generated from wild type alternatively spliced p53 RNA in mouse epidermal cells. Mol. Cell. Biol. **14:**1698–1708.
30. **Lane, D. P.** 1992. p53, the guardian of the genome. Nature (London) **358:**15–16.
31. **Lane, D. P., and S. Benchimol.** 1990. P53: oncogene or anti-oncogene? Genes Dev. **4:**1–8.
32. **Lin, D., M. Fiscella, P. M. O'Connor, J. Jackman, M. Chen, L. L. Luo, A. Sala, S. Travali, E. Appella, and W. E. Mercer.** 1994. Constitutive expression of B-myb can bypass p53-induced WAF1/Cip 1-mediated G1 arrest. Proc. Natl. Acad. Sci. USA **91:**10079–10083.
33. **Livingstone, A., R. J. Mairs, J. Russell, J. O'Donoghue, M. N. Gaze, and T. E. Wheldon.** 1994. N-myc gene copy number in neuroblastoma cell lines and resistance to experimental treatment. Eur. J. Cancer **30A:**382–389.
34. **Livingstone, L. R., A. White, J. Sprouse, E. Livanos, T. Jacks, and T. D. Tlsty.** 1992. Altered cell cycle arrest and gene amplification potential accompany loss of wild-type p53. Cell **70:**923–935.
35. **Lu, X., and D. P. Lane.** 1993. Differential induction of transcriptionally active p53 following UV or ionizing radiation: defects in chromosome instability syndromes? Cell **75:**765–778.
36. **Martinez, J., I. Georgoff, J. Martinez, and A. J. Levine.** 1991. Cellular localization and cell cycle regulation by a temperature sensitive p53 protein. Genes Dev. **5:**151–159.
37. **McMillan, T. J., A. M. Cassoni, S. Edwards, A. Holmes, and J. H. Peacock.** 1990. The relationship of DNA double strand break induction to radiosensitivity in human tumor cell lines. Int. J. Radiat. Biol. **58:**427–438.
38. **Melino, G., M. Annicchiarico-Petruzelli, L. Piredda, E. Candi, V. Gentile, P. J. Davies, and M. Piacentini.** 1994. Tissue transglutaminase and apopto-

sis: sense and antisense transfection studies with human neuroblastoma cells. Mol. Cell. Biol. **14:**6584–6596.
39. **Michieli, P., M. Chedid, D. Lin, H. Pierce, W. E. Mercer, and D. Givol.** 1994. Induction of WAF1/CIP 1 by a p53-independent pathway. Cancer Res. **54:** 3391–3395.
40. **Mietz, J. A., T. Unger, J. M. Huibregtse, and P. M. Howley.** 1992. The transcriptional transactivation function of wild-type p53 is inhibited by SV40 large T-antigen and by HPV-16 E6 oncoprotein. EMBO J. **11:**5013–5020.
41. **Moll, U. M.** Unpublished data.
41a. **Moll, U. M., et al.** Unpublished data.
42. **Moll, U. M., M. LaQuaglia, J. Benard, and G. Riou.** 1995. Wild-type p53 protein undergoes cytoplasmic sequestration in undifferentiated neuroblastomas but not in differentiated tumors. Proc. Natl. Acad. Sci. USA **92:** 4407–4411.
43. **Moll, U. M., G. Riou, and A. J. Levine.** 1992. Two distinct mechanisms alter p53 in breast cancer: mutation and nuclear exclusion. Proc. Natl. Acad. Sci. USA **89:**7262–7266.
44. **Momand, J., G. P. Zambetti, D. C. Olson, D. George, and A. J. Levine.** 1992. The mdm-2 oncogene product forms a complex with the p53 protein and inhibits p53-mediated transactivation. Cell **69:**1237–1245.
45. **Negrini, M., S. Sabbioni, S. Haldar, L. Possati, A. Castagnoli, A. Corallini, G. Barbanti-Brodano, and C. Croce.** 1994. Tumor and growth suppression of breast cancer cells by chromosome 17-associated functions. Cancer Res. **54:** 1818–1824.
46. **Nelson, W. G., and M. B. Kastan.** 1994. DNA strand breaks: the DNA template alterations that trigger p53-dependent DNA damage response pathways. Mol. Cell. Biol. **14:**1815–1823.
47. **Noda, A., Y. Ning, S. F. Venable, O. M. Pereira-Smith, and J. R. Smith.** 1994. Cloning of senescent cell-derived inhibitors of DNA synthesis using an expression screen. Exp. Cell Res. **211:**90–98.
48. **Oliner, J. D., K. W. Kinzler, P. S. Meltzer, D. L. George, and B. Vogelstein.** 1992. Amplification of a gene encoding a p53-associated protein in human sarcomas. Nature (London) **358:**80–83.
49. **Oren, M., W. Maltzman, and A. J. Levine.** 1981. Posttranslational regulation of the 54K cellular tumor antigen in normal and transformed cells. Mol. Cell. Biol. **1:**101–110.
50. **Prives, C., J. Bargonetti, G. Farmer, E. Ferrari, P. Friedlander, L. Jayaraman, Y. Wang, N. Pavletich, and U. Hubscher.** 1994. DNA-binding properties of the p53 tumor suppressor protein. Cold Spring Harbor Symp. Quant. Biol. **59:**207–213.
51. **Sidell, N., and H. P. Koeffler.** 1988. Modulation of Mr 53,000 protein with induction of differentiation of human neuroblastoma cells. Cancer Res. **48:** 2226–2230.
52. **Scheffner, M., B. A. Werness, M. Huibregtse, A. J. Levine, and P. M. Howley.** 1990. The E6 oncoprotein encoded by human papillomavirus types 16 and 18 promotes the degradation of p53. Cell **63:**1129–1136.
53. **Shaulsky, G., A. Ben-Ze'ev, and V. Rotter.** 1990. Subcellular distributions of the p53 protein during the cell cycle of Balb/c 3T3 cells. Oncogene **5:** 1707–1711.
54. **Shaulsky, G., N. Goldfinger, A. Ben-Ze'ev, and V. Rotter.** 1990. Nuclear accumulation of p53 protein is mediated by several nuclear localization signals and plays a role in tumorigenesis. Mol. Cell. Biol. **10:**6565–6577.
55. **Shaulsky, G., N. Goldfinger, A. Peled, and V. Rotter.** 1991. Involvement of wild-type p53 protein in the cell cycle requires nuclear localization. Cell Growth Differ. **2:**661–667.
56. **Shaulsky, G., N. Goldfinger, M. Tosky, A. J. Levine, and V. Rotter.** 1991. Nuclear localization is essential for the activity of p53 protein. Oncogene **6:** 2055–2065.
57. **Speir, E., R. Modaki, E. S. Huang, M. B. Leon, F. Shawl, T. Finkel, and S. E. Epstein.** 1994. Potential role of human cytomegalovirus and p53 interaction in coronary restenosis. Science **265:**391–394.
58. **Takahashi, K., H. Sumimoto, K. Suzuki, and T. Ono.** 1993. Protein synthesis-dependent cytoplasmic translocation of p53 protein after serum stimulation of growth-arrested MCF-7 cells. Mol. Carcinog. **8:**58–66.
59. **Takahashi, T., M. M. Nam, I. Chiba, M. J. Birrer, R. K. Rosenberg, M. Vinocour, M. Levitt, H. Pass, A. F. Gazdar, and J. D. Minna.** 1989. P53: a frequent target for genetic abnormalities in lung cancer. Science **246:**491–494.
60. **Ueda, H., S. J. Ullrich, J. D. Gangemi, C. A. Kappel, L. Ngo, M. A. Feitelson, and G. Jay.** 1995. Functional inactivation but not structural mutation of p53 causes liver cancer. Nat. Genet. **9:**41–44.
61. **Wagner, I., H. Arlt, L. van Dyck, T. Langer, and W. Neupert.** 1994. Molecular chaperones cooperate with PIM 1 protease in the degradation of misfolded proteins in mitochondria. EMBO J. **13:**5135–5145.
62. **Wang, X. W., K. Forrester, H. Yeh, M. A. Feitelson, J.-R. Gu, and C. C. Harris.** 1994. Hepatitis B virus X protein inhibits p53 sequence-specific DNA binding, transcriptional activity and association with transcription factor ERCC 3. Proc. Natl. Acad. Sci. USA **91:**2230–2234.
63. **White, E.** 1994. P53, guardian of Rb. Nature (London) **371:**21–22.
64. **Vindelov, L. L., I. J. Christensen, and N. I. Nissen.** 1983. A detergent-trypsin method for the preparation of nuclei for flow cytometric DNA analysis. Cytometry **3:**323–327.
65. **Vojtesek, B., and D. P. Lane.** 1993. Regulation of p53 protein expression in human breast cancer cell lines. J. Life Sci. **105:**607–612.
66. **Wu, X., J. H. Bayle, D. Olson, and A. J. Levine.** 1993. The p53-mem2 autoregulatory feedback loop. Genes Dev. **7:**1126–1132.
67. **Xiong, Y., G. J. Hannon, H. Zhang, D. Casso, R. Kobayashi, and D. Beach.** 1993. P21 is a universal inhibitor of cyclin kinases. Nature (London) **366:** 701–704.
68. **Yew, P. R., and A. J. Berk.** 1992. Inhibition of p53 transactivation required for transformation by adenovirus early 1B protein. Nature (London) **357:** 82–85.
69. **Yewdell, J. W., J. V. Gannon, and D. P. Lane.** 1986. Monoclonal antibody analysis of p53 expression in normal and transformed cells. J. Virol. **59:** 444–452.
70. **Yin, Y., M. A. Tainsky, F. Z. Bischoff, L. Z. Strong, and G. M. Wahl.** 1992. Wild-type p53 restores cell cycle control and inhibits gene amplification in cells with mutant p53 alleles. Cell **70:**937–948.

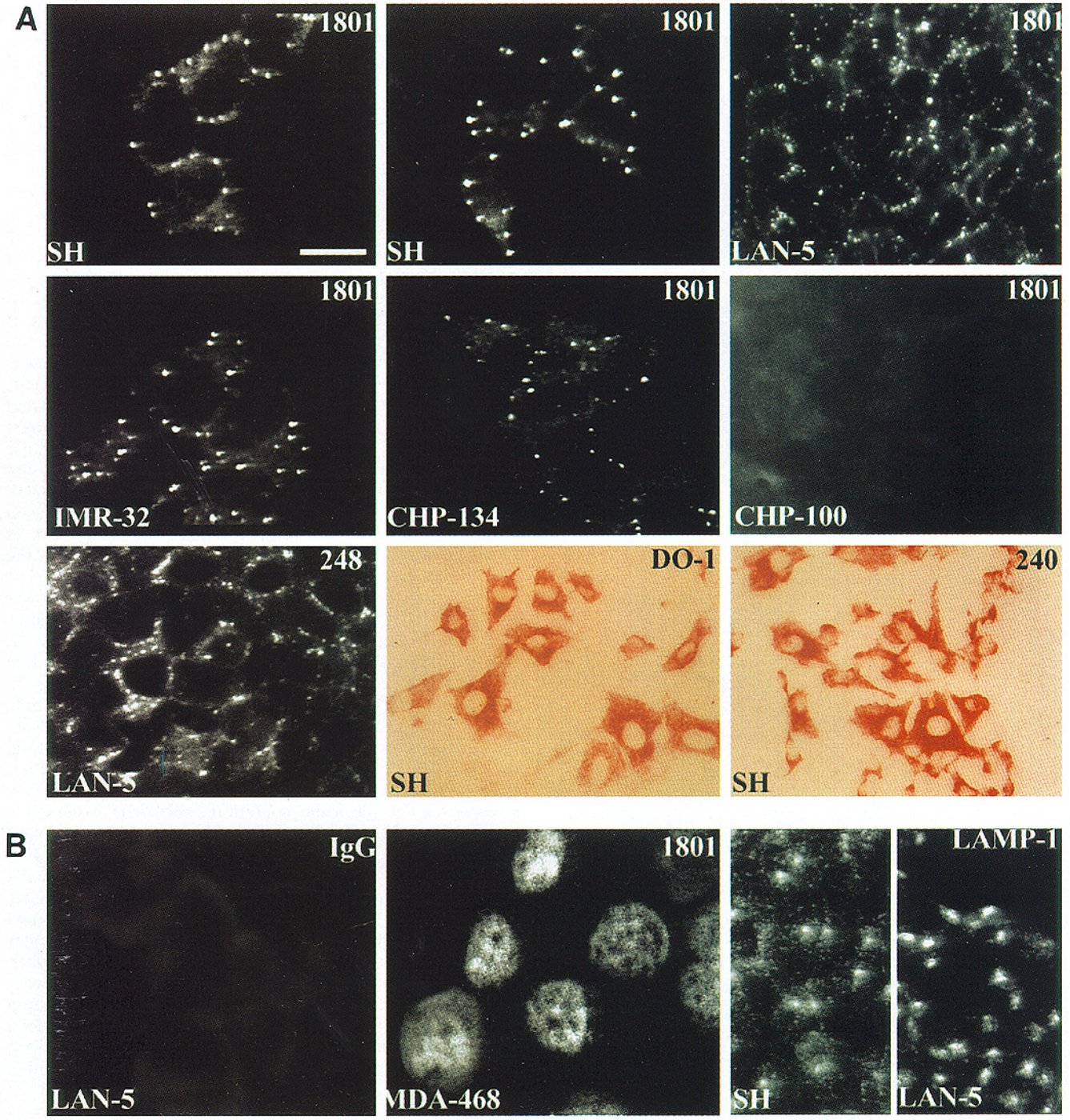
A
1801
SH
1801
SH
1801
LAN-5
1801
IMR-32
1801
CHP-134
1801
CHP-100
248
LAN-5
DO-1
SH
240
SH
B
IgG
LAN-5
1801
MDA-468
SH
LAMP-1
LAN-5

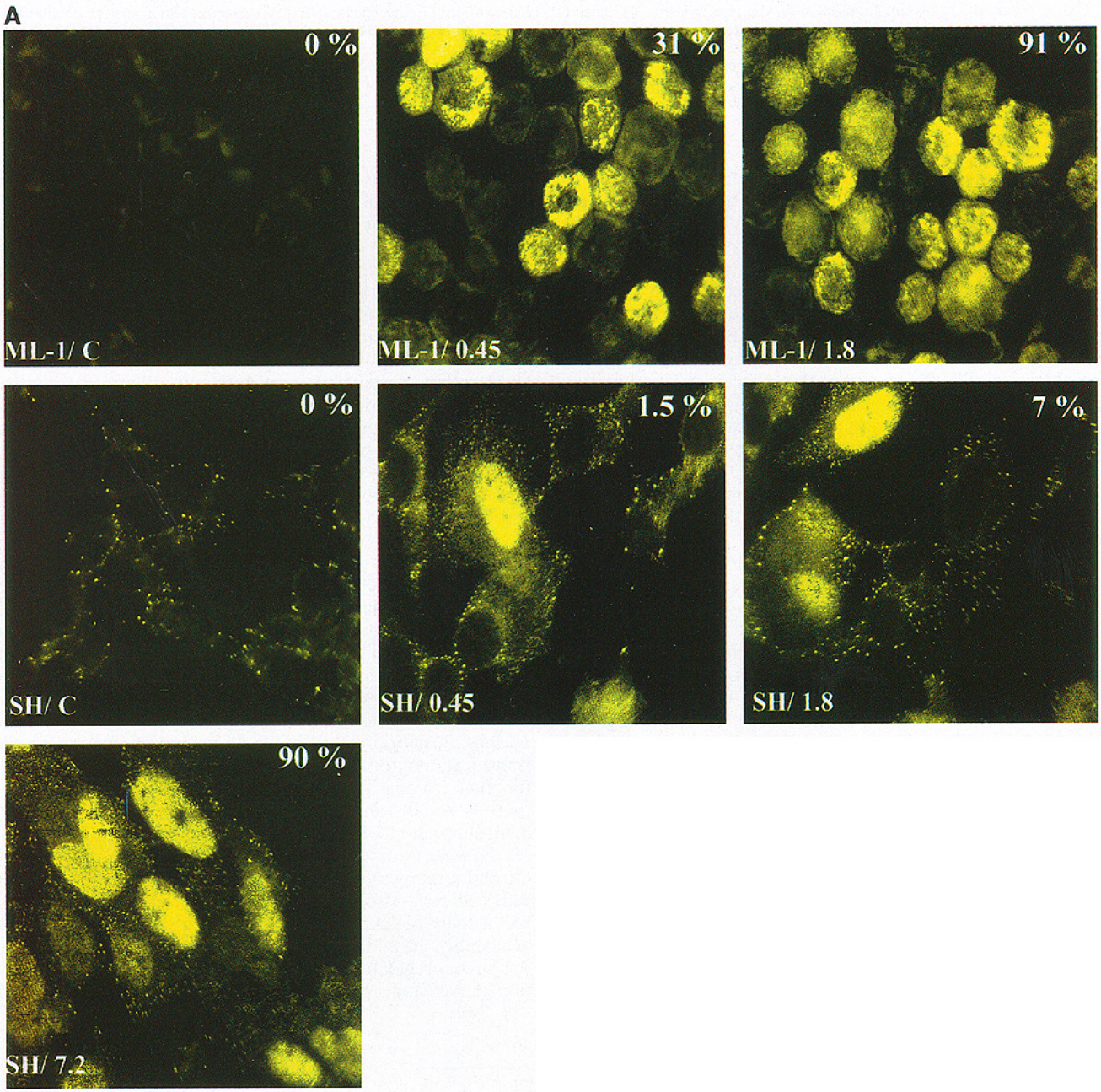
A
0 %
ML-1/ C
31 %
ML-1/ 0.45
91 %
ML-1/ 1.8
0 %
SH/ C
1.5 %
SH/ 0.45
7 %
SH/ 1.8
90 %
SH/ 7.2